

# OPTIMIZATION OF HIGH ANGLE-OF-ATTACK APPROACH AND LANDING TRAJECTORIES

**H.G. Visser**  
**Faculty of Aerospace Engineering**  
**Delft University of Technology**  
**Delft, The Netherlands**

**Keywords:** *ESTOL, trajectory optimization, thrust vectoring*

## Abstract

*The use of thrust vectoring technologies for performing extremely short takeoff and landing (ESTOL) operations was recently successfully demonstrated in a series of flight experiments involving the X-31 aircraft.*

*The study presented herein builds on these ESTOL developments. More specifically, the main goal of the present study is to shape high angle-of-attack approach trajectories in such a way that, starting at a given altitude and speed, the down-range distance to the runway threshold is minimized. In other words, we seek the steepest approach possible.*

*The approach to landing problem is formulated as an optimal control problem and solved numerically, using a rigid body model of a thrust-vectoring version of an F-16 fighter aircraft. The employed numerical method, collocation with nonlinear programming, proves well suited for solving this problem.*

## 1 Introduction

In May 2003 an extensive multinational flight test program aimed at demonstrating the use of thrust vectoring technologies for performing extremely short takeoff and landing (ESTOL) operations was successfully concluded [1]. The main goal of the ESTOL flight experiments was to explore how extremely short-landing capabilities could be exploited to increase military aircraft safety and operational flexibility. The main benefits of an ESTOL-capable aircraft include the ability to land on

carrier decks at speeds lower than current aircraft can, reducing aircraft wear-and-tear and lowering carrier arresting gear and catapult maintenance requirements. Since thrust vectoring is an essential capability needed to enable ESTOL operation, the X-31 experimental aircraft was selected for the ESTOL demonstrations. In the ESTOL experiments, the X-31 demonstrated a series of fully automated landings on an actual runway, approaching at twice the normal angle-of-attack. The aircraft's thrust setting was set fairly high to generate sufficient thrust for vectoring. As a result, a 30% reduction in landing speed was obtained. In [2] it is shown that this significantly lower approach-to-landing speed results in a substantial landing distance reduction

The present trajectory optimization study builds on the ESTOL developments outlined above. More specifically, the main goal of the present study is to shape the high angle-of-attack approach trajectory in such a way that, starting at a given altitude and speed, the down-range distance to the runway threshold is minimized, while taking into account all safety and operational requirements. In other words, we seek the steepest approach possible. This type of approach might be of interest e.g. when operating in a hostile environment or in mountainous terrain.

The sequence of events in the steep high angle-of-attack approach is shown in Fig. 1. The aircraft will transition to the high angle-of-attack steep approach at an altitude of 1,000 m. at a distance  $x_0$  from the runway threshold. The descent eventually becomes shallower as the

runway gets nearer. Once the tail of the aircraft is 1 m off the runway, the aircraft is de-rotated, while the tail maintains the 1-m clearance using thrust vectoring. After touchdown, a ground run takes place during which the aircraft is decelerated to a complete stop. The rollout phase is also included in the problem formulation.

In this paper, the steep high angle-of-attack approach to landing problem is formulated as an optimal control problem and solved numerically. The optimal control problem formulation is preceded by a brief description of the physical modeling. Several numerical examples, involving an F-16 type aircraft, are presented and the characteristic features of the approach trajectories are discussed.

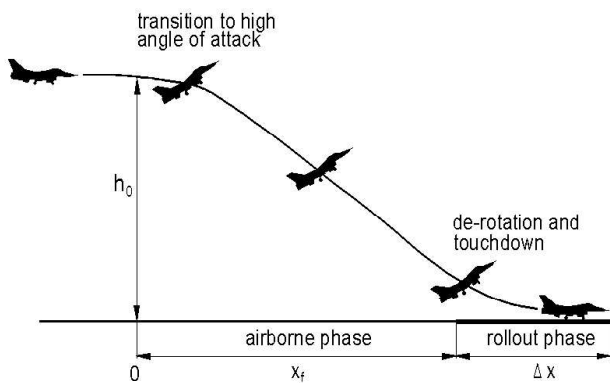


Fig. 1 Sequence of Events

## 2 Physical Modeling

The equations of motion are those for flight in a vertical plane over a flat non-rotating earth. Using a rigid-body model that considers the effects of thrust vectoring [3], the equations of motion can be written as:

$$\dot{x} = V \cos \gamma \quad (1)$$

$$\dot{h} = V \sin \gamma \quad (2)$$

$$\dot{V} = \frac{g}{W} (T \cos(\alpha + \epsilon_T) - C_D \bar{q} S - W \sin \gamma) \quad (3)$$

$$\dot{\gamma} = \frac{g}{WV} (T \sin(\alpha + \epsilon_T) + C_L \bar{q} S - W \cos \gamma) \quad (4)$$

$$\dot{q} = \frac{\bar{q} S \bar{c} C_m - T \sin \epsilon_T l_x}{I_{yy}} \quad (5)$$

$$\dot{\alpha} = q - \dot{\gamma} \quad (6)$$

where,  $x$  and  $h$  are the position coordinates,  $V$  is the airspeed,  $\gamma$  is the flight path angle,  $q$  is the pitch rate and  $\alpha$  is the angle-of-attack. The dynamic pressure is:

$$\bar{q} = \frac{1}{2} \rho V^2 \quad (7)$$

The aircraft's motion is governed by three independent control variables, the thrust  $T$ , the elevator angle  $\delta_e$ , and the thrust vector angle  $\epsilon_T$ , which are subject to the following constraints:

$$T_{min} \leq T \leq T_{max} \quad (8)$$

$$\delta_{e_{min}} \leq \delta_e \leq \delta_{e_{max}} \quad (9)$$

$$\epsilon_{T_{min}} \leq \epsilon_T \leq \epsilon_{T_{max}} \quad (10)$$

The maximum thrust is assumed to be a (linear) function of altitude ( $h$ ) and Mach number ( $M$ ):

$$T_{max} = T_0 + T_h \cdot h + T_M \cdot M \quad (11)$$

In addition to the above control constraints, there are a number of state constraints and mixed state/control constraints. First of all, the angle-of-attack is limited:

$$\alpha(t) \leq \alpha_{max} \quad (12)$$

Secondly, it is assumed that the normal load factor  $n_z$  is constrained:

$$n_z(t) \leq n_{max} \quad (13)$$

where the load factor  $n_z$  is defined as [3]:

$$n_z = \frac{g}{W} (T \sin \epsilon_T + C_L \bar{q} S \cos \alpha + C_D \bar{q} S \sin \alpha) \quad (14)$$

Finally, there is the requirement that the tail height  $h_{tail}$  should be kept at or above the ground

clearance height  $h_{min}$  (which in this study is assumed to be 1 m):

$$h_{tail} = h - l_x \sin\theta \geq h_{min} \quad , \quad (15)$$

where  $l_x$  is the distance from the thrust vectoring system to the center of gravity, and  $\theta (= \alpha + \gamma)$  is the pitch attitude.

The density variation  $\rho(h)$  is based on the U.S Standard Atmosphere, 1962 [4].

The aerodynamic coefficients employed in this study relate to a conventional (non-thrust-vector) F-16 model and are derived from [5]. The data presented in [5] is for an F-16 flying at relative low Mach numbers ( $< 0.6$ ), out of ground effect, with landing gear retracted, and no external stores. No modifications to allow for ground effect or thrust-vector system installation effects have been introduced in this research. However, to correct for the extended undercarriage, an additional drag term  $\Delta C_{D_{uc}}$  has been included in the aerodynamic drag model:

$$C_D = -C_X \cos\alpha + C_Z \sin\alpha + \Delta C_{D_{uc}} \quad (16)$$

The lift coefficient  $C_L$  is given by:

$$C_L = C_X \sin\alpha - C_Z \cos\alpha \quad (17)$$

In Eqs. (16) and (17) the following expressions for the non-dimensional aerodynamic force coefficients  $C_X$  and  $C_Z$  have been used [5]:

$$C_X = C_{X_0}(\alpha, \delta_e) + C_{X_q}(\alpha) q \bar{c} / 2V \quad (18)$$

$$C_Z = C_{Z_0}(\alpha, \delta_e) + C_{Z_q}(\alpha) q \bar{c} / 2V \quad , \quad (19)$$

with  $\bar{c}$  the wing reference chord. Similarly, the expression for the non-dimensional aerodynamic moment coefficient  $C_m$  is given by:

$$C_m = C_{m_0}(\alpha, \delta_e) + C_{m_q}(\alpha) q \bar{c} / 2V \quad (20)$$

### 3 Flight Path Optimization

#### 3.1 Boundary Conditions

The primary objective in the flight path optimization problem to be solved concerns the down-range distance to the runway threshold (see Fig. 1). In order not to compromise the down-range criterion, no boundary condition for the touchdown speed is imposed. However, to ensure a safe landing, the vertical speed at touchdown is restricted and also the allowable pitch attitude at touchdown is limited to a specified range:

$$\dot{h}_{max} \geq \dot{h}(t_f) \geq \dot{h}_{min} ; 0 \leq \theta(t_f) \leq \theta_{max} \quad (21)$$

At the initial time  $t_0$ , boundary conditions are specified for all state variables. The final boundary conditions (21) are complemented with the requirement:

$$h(t_f) = h_f (= 2 m) \quad (22)$$

#### 3.2 Performance Index

The primary performance index is, as stated, the down range distance. However, to allow for the fact that no boundary condition on the touchdown speed has been prescribed, the stopping distance after touchdown  $\Delta x$  is included in the overall performance index (see Fig.1):

$$J = x_f + \Delta x \quad , \quad (23)$$

with:

$$\Delta x = - \frac{V_f^2}{2a} \quad (24)$$

Note that the aircraft is assumed to decelerate at a constant rate  $a$  in the ground run. In this study, it is assumed that along the runway the aircraft decelerates at  $-2.5g$ , a typical value for an arresting gear landing [6]. From Eq.(24) it is readily clear that including the stopping distance  $\Delta x$  in the performance index essentially boils down to adding a

quadratic penalty term involving the touchdown speed.

### 3.2 Numerical Method.

In this study the *direct* optimization technique of collocation with nonlinear programming [7] has been used for the numerical resolution of the flight path optimization problem. In this approach, the representation of control variables as functions of time is reduced to choosing an appropriate finite set of parameters. Nonlinear programming is then used to select the parameters such as to minimize the defined objective function. The collocation approach adopted herein requires discretization of the trajectory dynamics. The discrete dynamics along with the path-constraints are then treated as algebraic inequalities to be satisfied by the nonlinear program (implicit integration).

To perform the optimal trajectory calculations, a software package called *Ezopt* has been used [8]. This package proved to be quite capable of dealing with the massive non-linear program that emerges as a result of the rather small collocation step size that is adopted. A small collocation step size is required in order to be able to capture the fast rotational dynamics.

## 4 Numerical Results

Optimal flight paths have been generated for various combinations of initial conditions and also for several values of the minimum thrust setting. Unlike in the ESTOL experiments, where the thrust setting is set fairly high to generate sufficient thrust for vectoring, the minimum thrust setting plays an important role in shaping the steep approach trajectories. It is readily clear that, in order to bleed off excess speed at a high rate, thrust settings are typically set at the lower limit for large parts of the trajectory.

In all presented numerical examples the following initial conditions are assumed:

$$\begin{aligned} x(t_0) &= 0 ; h(t_0) = 1,000 \text{ m} ; \gamma(t_0) = 0 \text{ rad} \\ \alpha(t_0) &= 0.15 \text{ rad} ; q(t_0) = 0 \text{ rad/s} \end{aligned}$$

Also, the constraint values for the terminal constraints (21) are the same in all numerical examples:

$$\begin{aligned} \dot{h}_{\max} &= -0.5 \text{ m/s} ; \dot{h}_{\min} = -2.5 \text{ m/s} \\ \theta_{\max} &= 0.2 \text{ rad} \end{aligned}$$

The load factor limit  $n_{\max}$  has been set at 1.5 in the numerical examples. Unless explicitly stated differently, the minimum thrust setting is taken as:

$$T_{\min} = 0.4 T_{\max} \quad (26)$$

In all examples, a maximum angle-of-attack of  $45^\circ$  has been assumed ( $\alpha_{\max} = 0.7854$  rad). The remaining parameters of the physical model (F-16) are listed in Appendix A.

Numerical results for the first case, which relates to an initial speed  $V(t_0) = 100$  m/s, are presented in Fig.2. The optimal trajectory is characterized by three different flight phases. In the initial phase, the aircraft transitions to high-angle of attack. The ‘‘cobra-like’’ [3] pull-up maneuver results in a significant increase in altitude, while speed drops off dramatically. In the initial seconds of the maneuver, the increase in angle-of-attack is limited by the normal load factor constraint. In the second (post-stall) phase, the aircraft more or less settles in steady state, at a speed, which is about half the initial speed. In this steady state phase, the aircraft descends at a fairly high rate and at the minimum thrust setting. Finally, in the third phase the aircraft transitions from a post-stall condition to a conventional landing attitude. The de-rotation takes place quite rapidly during the final few seconds before touchdown. At touchdown the rate-of-descent is within the permissible range.

Fig. 3 shows some more detailed results of the flare maneuver for the same case as considered in Fig. 2. The two altitude histories shown in Fig.3 relate to the center of gravity (c.g.) and the tail, respectively.

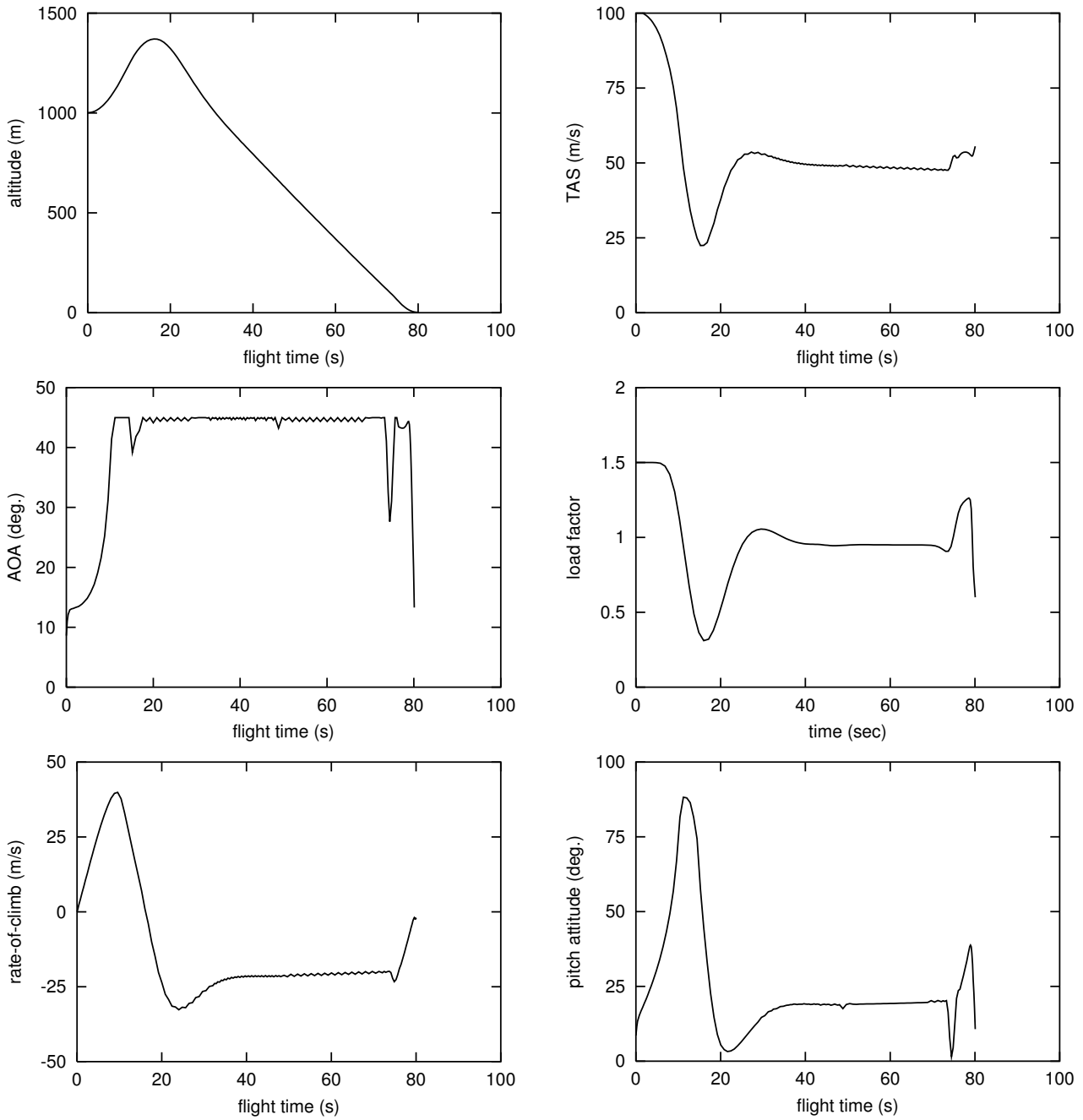


Fig. 2 Optimal Trajectory Results for the Case with  $V(t_0) = 100$  m/s

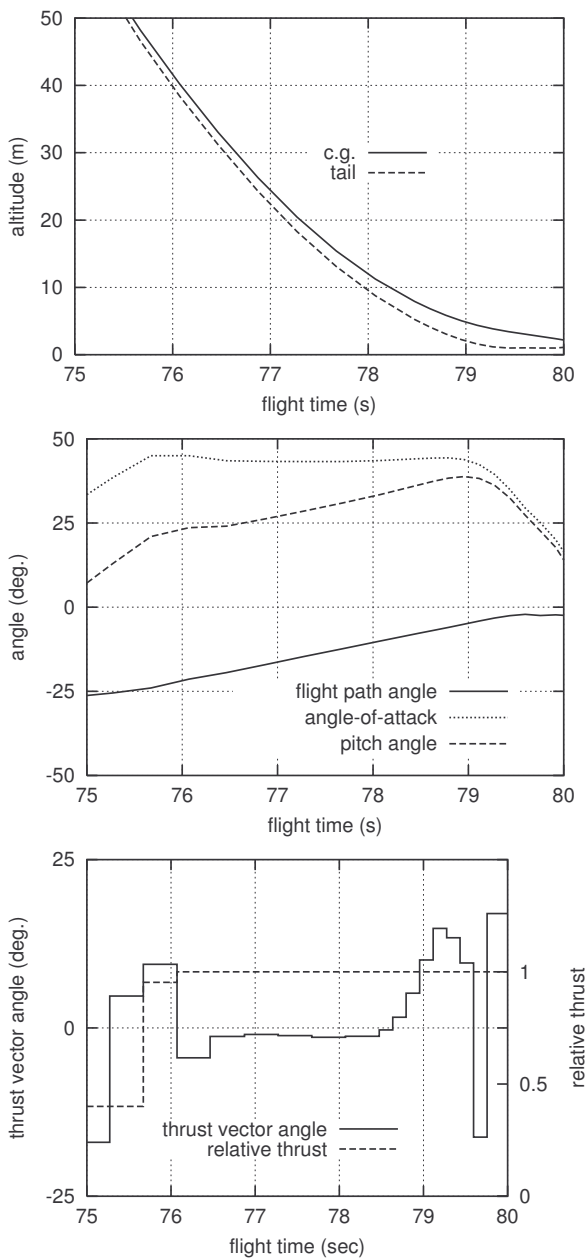


Fig. 3 Detailed Trajectory Results for the Case with  $V(t_0) = 100$  m/s.

Close to touchdown, both the tail clearance constraint and the pitch attitude constraint are active. At the start of the flare (i.e., final 4 seconds of the flight), thrust is increased to its maximum setting.

Note that in Fig. 3 the history of relative thrust (i.e.,  $T/T_{max}$ ) is provided. When the thrust level is increased, the thrust vectoring activity is reduced until the actual de-rotation occurs. The

de-rotation from maximum angle-of-attack to the landing attitude essentially takes place during the final second of the flight. De-rotation is activated by increasing the thrust vector angle. The decrease in angle-of-attack reduces lift. However, the thrust deflection partly compensates for this loss. Speed is slightly increased during the de-rotation.

Since thrust is at its lower limit during the largest part of the flight, a performance improvement is to be expected when the permissible value of the lower limit is further reduced. Fig. 4 shows some results for various values of the minimum thrust setting. From the results in Fig. 4 it is readily clear that the value of the lower thrust limit does indeed have a significant impact.

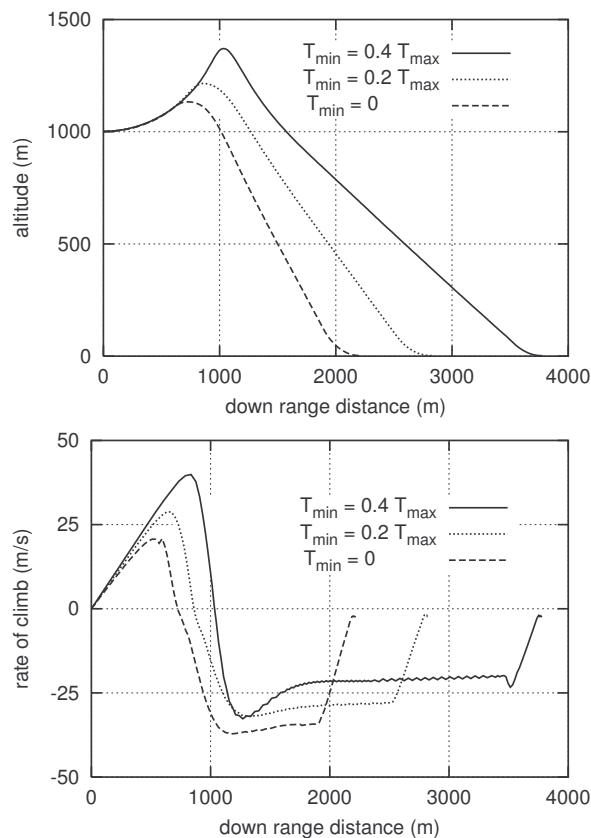


Fig. 4 Trajectory Results for Various Minimum Thrust Settings.

It is readily clear that in order for thrust vectoring to be effective, a sufficient level of thrust must be provided. Setting the thrust

setting to zero may be favorable from a performance perspective, but at the same time it also incapacitates the thrust vectoring control system. When low minimum thrust settings are permitted, the optimization process attempts to establish an optimal compromise between the two conflicting requirements of path performance and control effectiveness. Fig. 5 shows histories for relative thrust (i.e.,  $T/T_{max}$ ) for several values of the minimum thrust setting, for a certain timeframe.

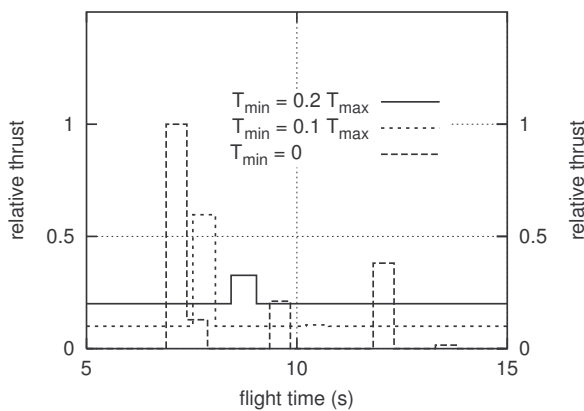


Fig. 5 Relative Thrust Histories for Various Minimum Thrust Settings.

When the permissible lower value of thrust is taken as zero, the optimal setting of thrust will be on this lower limit. Occasionally, thrust pulses that are large in magnitude but short in duration are commanded to provide the required thrust vector control input, while ensuring that the path performance is not affected too much. The higher the minimum thrust level, the lower the magnitude of the thrust pulses. When the minimum thrust level is taken larger than about  $0.3 T_{max}$ , the thrust pulses completely disappear and apparently the minimum thrust level is then sufficient to provide the required thrust vectoring control capability for the entire approach trajectory. Avoiding the need to adjust thrust setting during the approach is actually the primary reason for selecting the relative high minimum thrust setting assumed in (most of) the presented example cases.

Although thrust adjustments during the approach are not required, there still is the

virtually instantaneous change in thrust setting during the final seconds of the flare. The presently employed model does not allow for engine spool-up delays and therefore a model refinement is clearly warranted for future research.

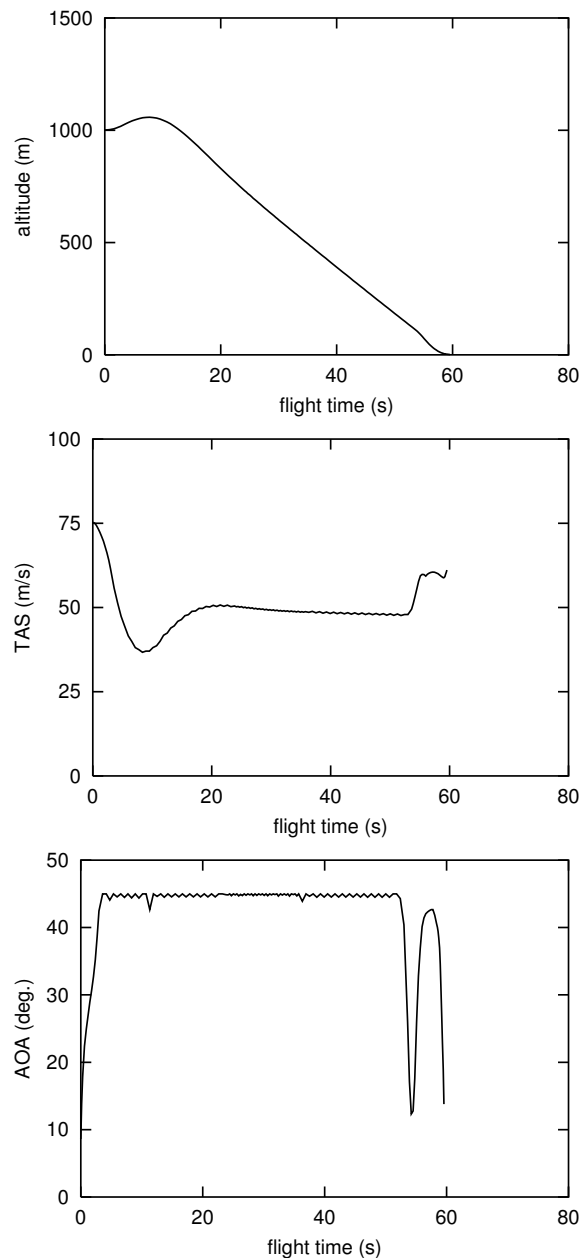


Fig. 6 Optimal Trajectory Results for the Case with  $V(t_0) = 75$  m/s.

It needs to be noted that the established optimal thrust control behavior is not really desirable from an operational and safety

perspective and additional constraints probably need to be introduced in a refined problem formulation.

The final numerical example addresses the influence of the initial speed on trajectory behavior. In the example presented in Fig. 2, the initial speed was taken as 100 m/s. To bleed off the excess speed a rather “violent” pitch up maneuver was required. In the final example, a much lower initial speed is assumed. The results for the case with initial speed  $V(t_0) = 75$  m/s, are presented in Fig. 6.

Inspection of Fig. 6 reveals that the lower initial speed does not result in a trajectory with significantly different characteristics. However, in comparison with the high initial speed maneuver considered in Fig. 2, the present maneuver is significantly more moderate in behavior. In particular, the initial increase in altitude is more moderate and also the speed undershoot is far less pronounced.

From a path performance perspective, a low initial speed is rather advantageous. The required distance to the runway threshold is indeed reduced by about 1 km in comparison to the high initial speed case.

## 5 Conclusions

In this paper the problem of a steep high angle-of-attack approach to landing has been formulated as an optimal control problem. A rigid-body model is used for the aircraft along with slightly modified aerodynamics of a (non-thrust-vectoring) F-16. A fairly detailed parameter study has been undertaken to establish the characteristics of the optimal trajectories that take into account a wide range of operational constraints. Optimal path performance typically requires that the approach trajectory be flown at minimum thrust. Only during the flare maneuver thrust is increased, thus providing the capability to de-rotate the aircraft by thrust vectoring. The bang-bang type thrust control behavior during the flare is not desirable from both an operational and modeling point of view and therefore requires further study.

## References

- [1] <http://www.aviationnow.com/content/publication/awst/20010305/aw38.htm>.
- [2] Selmon JR., White SN, Sheen JH, Bass DI, and Miranda L. High Angle of Attack Autonomous Landing Using the X-31A aircraft. *AIAA Guidance, Navigation, and Control conference*, Montreal, Canada, AIAA 2001-4207, 2001.
- [3] Komduur HJ and Visser HG. Optimization of Pitch Reversal Standard Agility Comparison Maneuvers. *Journal of Guidance, Control and Dynamics*, Vol. 25, No. 4, pp 693-702, 2002.
- [4] Ruijgrok GJJ. *Elements of Airplane Performance*. 1st edition, Delft University Press, Delft, The Netherlands, 1990.
- [5] Morelli EA. Global Nonlinear Parametric Modeling with Application to F-16 Aerodynamics. *American Control Conference*, Philadelphia, U.S.A., Vol. 2, pp. 997-1001, 1998.
- [6] Roskam J. *Airplane design – Part IV: Layout Design of Landing Gear and systems*. 2nd edition Roskam Aviation and Engineering Corporation, 1989.
- [7] Hargraves CR and Paris, SW. Direct Trajectory Optimization using Nonlinear Programming and Collocation. *Journal of Guidance, Control and Dynamics*, Vol. 25, No. 4, pp 780-785, 1987.
- [8] <http://www.ama-inc.com>.

## Appendix A: F-16 Model parameters

The following presents an overview of some important parameters of the F-16 fighter aircraft, along with some parameters used in the optimization. It needs to be noted that some of the parameter values are not based on exact data, but merely represent “guesstimates”. The weight  $W$  is 91200 N, the wing surface area  $S$  is 28.87 m<sup>2</sup>, the wing reference chord  $\bar{c}$  is 3.45 m, the moment of inertia  $I_{yy} = 75250$  kg.m<sup>2</sup>, the distance from the thrust vectoring system to the c.g.  $l_x$  is 4.5 m. The vertical speeds limits at touchdown are, respectively,  $\dot{h}_{\max} = -0.5$  m/s and  $\dot{h}_{\min} = -2.5$  m/s. The thrust coefficients are  $T_0 = 84500$  N,  $T_h = -8$  N/m,  $T_M = 30000$  N. The drag correction for undercarriage extension  $\Delta C_{D_{vc}}$  is estimated as 0.02. Finally, the control constraints are, respectively,  $\varepsilon_{T_{\max}} = 0.29670$  rad,  $\varepsilon_{T_{\min}} = -0.29670$  rad,  $\delta_{e_{\max}} = 0.4363$  rad and  $\delta_{e_{\min}} = -0.4363$  rad.